Resonance-Amplified Diffraction Sensors

Undergraduate Researcher
Jennifer Roden, Eastern Illinois University

Faculty Adviser
Joseph T. Hupp
Department of Chemistry,
Northwestern University

Graduate Student Mentor
Mohammed Parpia
Department of Chemistry,
Northwestern University

Abstract

The need to improve sensing technology for widespread application in everyday life is fueling the development of diffraction-based sensing, an optical sensing technique. Selectivity and sensitivity issues must first be resolved. Both selectivity and sensitivity can be increased by using resonance conditions — that is, using a probe wavelength where the system absorbs. The resonance effects are based on a change in absorbance that produces a surprisingly large but indirect change in the real part of the refractive index, as modeled by the Kramers-Kronig equation. In the two approaches studied here, the systems undergo absorbance changes upon analyte exposure. The first approach was aimed at development of a sensitive alcohol sensor through incorporation of CR-546, a chromoreactand dye, into a polymeric diffraction grating. This attempt was abandoned once theoretical results from the Kramers-Kronig equation showed the overall change in the real part of the refractive index was too small for detection. The second approach involved incorporation of silver nanospheres into an elastomer grating. These spheres have promising universal application due to the fact that absorbance changes in the quadrupolar coupling peak are accomplished with modulation in the refractive index. Theoretical results, based on unpatterned PDMS membranes, are promising. Incorporation of silver nanospheres in a diffraction grating was successfully attempted, but time restrictions prevented collection of diffraction data.

Introduction

Sensors are used in everyday life in numerous ways. They monitor air quality and detect chemical and biological agents that affect human health and health care. Unfortunately, the large-scale deployment of sensors is complicated by issues of selectivity, sensitivity, cost, reliability, size, usability, and durability.[1] Optical sensors have the potential to be low-cost, sensitive, and universally usable sensors because they rely on the modulation of the refractive index. Diffraction-based sensors are a type of optical sensor that has been used to detect bacteria,[2,3] proteins,[4] [$H3O^+$],[5] and volatile organic compounds (VOCs).[6] As expected, these sensors, while sensitive, have limited selectivity. Both selectivity and sensitivity can be increased in these systems by using resonance conditions — that is, using a probe wavelength where the system absorbs.[7] Two methods of signal amplification using resonance conditions are discussed separately in this paper: incorporating a chromoreactand dye in a polymeric grating and embedding silver nanospheres in an elastomer.

Background

Diffraction occurs when coherent light interacts with a substrate patterned with a periodic variation in refractive index ($\tilde{n}$), which is the sum of a real (n) and an imaginary component (k) that are both dependent on the position, x, and probe wavelength, λ.[1]

$$\tilde{n}(x,\lambda) = n(x,\lambda) + ik(x,\lambda)$$

The real component is related to the speed of light through the medium, while the imaginary component relates to the absorbance:

$$k = \frac{2.3\lambda OD}{4\pi}$$

where OD is the optical density and d is the grating thickness.[7]

The resulting diffraction pattern is related to the diffraction grating via a Fourier transform, as shown in Figure 1. A ratio of the intensities of the first diffraction spot, I_1, and undiffracted spot, I_0, is known as the diffraction efficiency (DE).[8]

$$DE = \frac{I_{0,1}}{\sum I_i} \approx \frac{I_{0,1}}{I_{0,0}}$$

The DE value depends on the refractive index contrast of the grating, $\tilde{n}_2 - \tilde{n}_1$, as illustrated in Scheme 1, which also summarizes the methodology of diffraction. Analyte binding to the patterned areas of the grating increases the refractive index of these areas $\tilde{n}_2$, since air ($\tilde{n}$~1) is displaced. The new refractive index contrast, $\tilde{n}_2' - \tilde{n}_1$, results in a new DE value, $DE_{analyte}$. The difference between the $DE_{analyte}$ and DE is used to model a percent change in the system, $\Delta DE\%$.[6,7]

$$\Delta DE\% = \frac{(DE_{analyte} - DE_0)}{DE_0} \times 100\%$$

Graphing $\Delta DE\%$ versus time results in a sensing curve. Four such curves are plotted in Figure 2. The toluene plot stands apart from the other three VOCs because of its selectivity and sensitivity. Unfortunately, neither selectivity nor

sensitivity is seen to any great degree in the other VOCs, severely restricting diffraction-based sensors' versatility.[6]

Improvements in selectivity and sensitivity can be achieved by using resonance conditions, in which a probe wavelength is used where the system absorbs.[8] In actuality, resonance amplification is only seen when the probe wavelength observes a change in absorbance. Since the imaginary component of the refractive index is dependent on the optical density, it is clear that resonance conditions would affect it. In contrast, the real component's dependence on absorption changes is indirect and is modeled by Kramers-Kronig equation:[8]

$$\Delta n(\omega') = \frac{c}{\pi} \int_0^\infty \frac{\Delta \alpha(\omega)}{\omega^2 - \omega'^2} d\omega$$

where $\Delta\alpha(\omega)$ is the change in absorptivity due to analyte exposure, and ω is the angular frequency ($\omega = 2\pi c/\lambda$). This indirect change of the real component is surprisingly large and forms the basis of resonance amplification.

Since resonance changes occur when absorbance changes, the two techniques, discussed separately here — incorporation of a chromoreactand dye and plasmon resonance — were chosen based on their ability to undergo absorbance shifting upon analyte exposure.

Chromoreactand Dye

Background

Gerhard Mohr and coworkers have synthesized a series of chromoreactand dyes.[9,10] The term *chromoreactand* was formed based on the absorbance shift due to reaction of the dye. One chromoreactand, CR-546, reacts with alcohols and amines to form hemiactal or a hemiaminal group from a trifluoroacetyl group, resulting in a change of λ_{max} from 560 nm to 480 nm.[10]

Approach

Incorporation of CR-546 into a poly(vinylchloride) (PVC) grating was attempted using soft lithographic techniques such as micromolding in capillaries. The grating also contained other compounds, in mixture ratio previously reported, that functioned as a plasticizer and catalyst.[10] Experimental comparison of two gratings, one fabricated with CR-546 and one without, was conducted. Ideally, this would show resonance amplification in the CR-546 presence at certain probe wavelengths. Two probe wavelengths were studied, 543 nm and

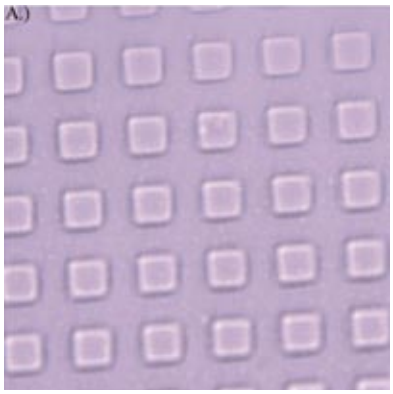

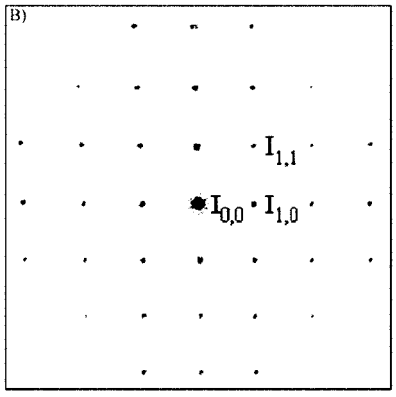

Figure. 1: The relationship of a diffraction grating (1A) and the diffraction pattern (1B) is based on a Fourier transformation. The grating shown here is composed of 5 µm polymer squares with 5 µm separation. The diffraction pattern pictured here shows the labeling of the diffraction spots whose ratio is used to define the diffraction efficiency, DE. (1B reprinted with permission.[7] © 2002 American Chemical Society.)

633 nm, using ethanol and toluene vapor. Toluene exposure was used to show that signal amplification occurred only with a CR-546 reactive analyte.

Modeling using the Kramers-Kronig equation was conducted using UV-Vis spectra collected on a 15 µm thick membrane layer containing all the previously mentioned compounds.[10] The UV-Vis spectra collected were obtained in water and in a 20% v/v aqueous ethanol mixture.

Results and Discussion

The results from the diffraction study, consisting of two gratings — one with CR-546 and one without — were poor. Figure 3 shows the Δ graph of the grating containing no dye, which is extremely noisy. A graph of the grating containing CR-546 can be imagined to have ethanol amplification at certain probe wavelengths and no toluene amplification, but no such graph could be obtained experimentally. Such reasons as dye impurity, thin gratings, and a small change in absorbance would lead to poor diffraction results, as were obtained. The experimental UV-Vis spectra, shown in Figure 4, differed from the previously reported UV-Vis, supporting the use of impure dye.[10] The main difference between the spectra was that the reported trifluotoacetyl peak was much more defined before ethanol exposure, implying that less pure CR-546 was used. Additionally, the grating thickness, ~60nm, was significantly smaller than the 1 µm membranes used to observed the large absorbance change. Since the same ratio of components was used, the amount of CR-546 in the grating might not have been significant enough to obtain high resonance amplification. However, increased grating thickness would have severe repercussions for the response time, which is diffusion limited.

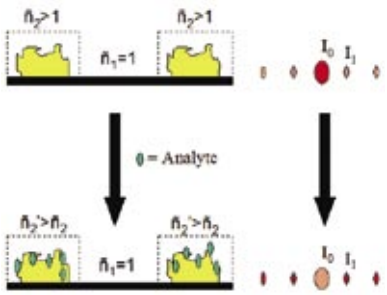

Scheme 1: The analyte interacts with the grating by displacing air, which increases the refractive index of the patterned regions, $\tilde{n}_2$. Additionally, a generic diffraction pattern is shown where the intensity of the diffracted spots increases and the undiffracted spot decreases upon analyte exposure. The change in intensities modifies the DE, allowing a percent change to be monitored over time. (Adapted.[15] © 2000 American Chemical Society.)

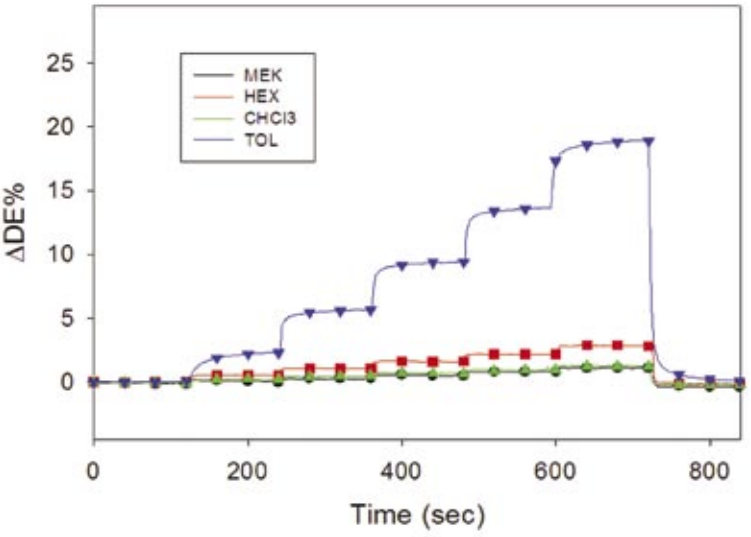

Figure 2: Four VOCs including toluene, methyl ethyl ketone, chloroform, and hexane are shown. The toluene shows sensitivity and selectivity; however, the other three compounds show no selectivity. (Their sensitivity can be increased by using different polymeric gratings.[6]) Resonance conditions can be used to increase the selectivity as well as sensitivity of a given system. (Reprinted with permission.[6] © 2003 American Chemical Society.)

Lastly, the large absorbance change was present in a 20% ethanol solution, and diffraction measurements were obtained in the vapor phase that most likely did not interact with the grating as strongly as in the liquid.

In order to gauge the capabilities of the experimental system, computational modeling was employed. The resulting Δn value was only on the order of magnitude of 10^{-5}, which is not large enough to be seen in the diffraction setup due to the system's noise (see Figure 3). Overall, it appeared that incorporation of the CR-546 into a grating would not result in changes in absorbance — and thus in Δn — large enough for effective resonance enhancement to occur.

Plasmon Resonance

Background

Plasmon resonance is the collective oscillation of conduction electrons in noble nano-sized metals such as gold, copper, and silver. The plasmon resonance of immobilized silver nanospheres has been investigated by George Chumanov and coworkers.[11,12] The quadrupolar coupling between these unpatterned, closely spaced immobilized silver spheres is observed in the visible region with a surprisingly narrow excitation peak at 436 nm whose λ_{max} is dependent on the refractive index environment.[12] Due to the narrowness of this peak, small shifts in λ_{max} caused by exposure to analytes would result in dramatic changes in $\Delta\alpha$ value. Thus, these spheres should be capable of causing large resonance amplification in diffraction gratings based on the Kramers-Kronig equation.

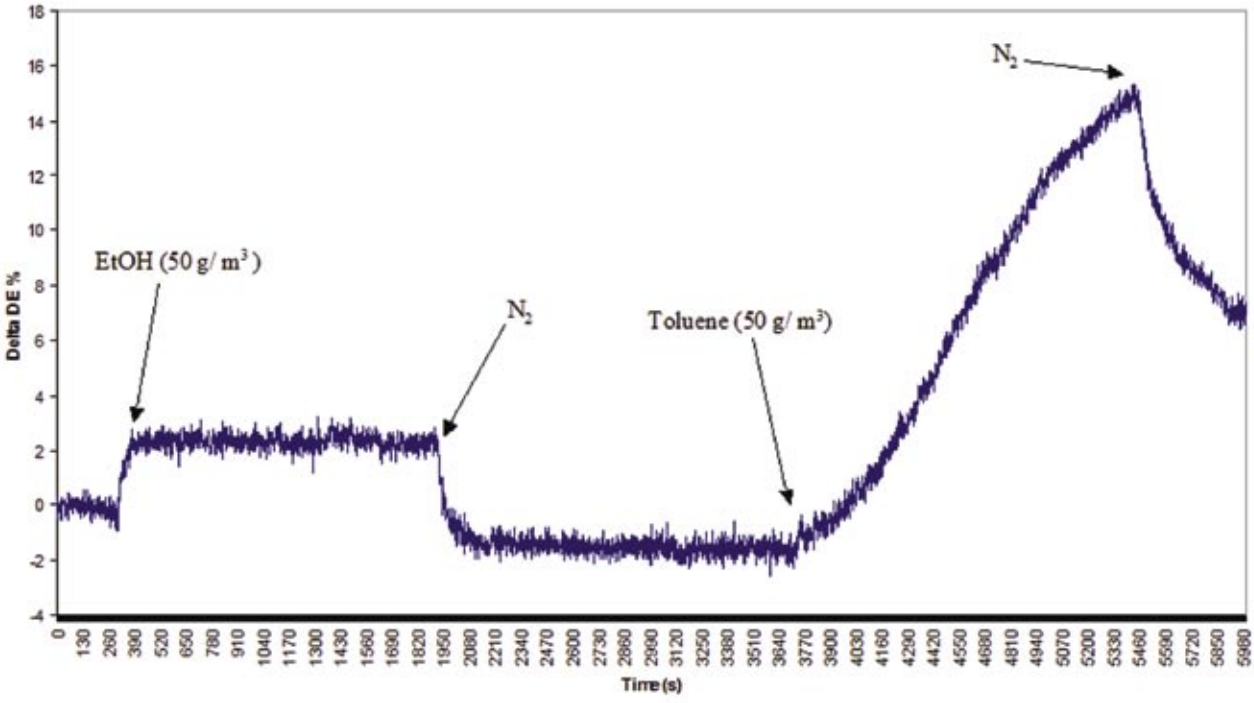

Figure 3: A plot of ΔDE% upon ethanol and toluene exposure to a grating containing no CR-546 is shown. The noise level is extremely high. In addition, no other plots could be collected possibly due to impure CR-546, too thin a grating, and a lack of ethanol interaction in the vapor phase.

Approach

Three reduction reactions were attempted in order to synthesize silver nanospheres of approximately 100 nm: sodium borohydride,[13] citrate,[13] and H_2 (g).[14] Immobilization of the silver nanospheres in poly(dimethylsiloxane) (PDMS) onto a functional silicon wafer was achieved via a two-step process. First, the spheres were immobilized onto a poly(vinylpyridine) (PVP) functionalized silicon wafer, which was then coated with PDMS. After curing, the PDMS was simply peeled away.[14] UV-Vis data of the membranes was collected to assist in determining not only sphere surface density, but also absorbance change upon acetone exposure. These absorbance spectra were then used for theoretical modeling using the Kramers-Kronig equation.

Immobilization of the silver nanospheres was then attempted in a patterned PDMS grating consisting of 10 µm channels. Initially, silicon wafers patterned photolithographically were functionalized with PVP. The spheres were than attached to this surface and removed after curing in PDMS, which had been poured over the wafer. SEM images of the patterned PDMS were collected.

Results and Discussion

All three reactions successfully synthesized silver nanospheres. However, both the sodium borohydride and citrate reactions produced polydisperse nanospheres with diameters less than 100 nm. The H_2 (g) reduction allowed a broad range of selective sphere sizes to be formed based on reaction time.[14] Also, the H_2 (g) reduction reaction resulted in a higher surface density because of its lower ionic strength solution.[12]

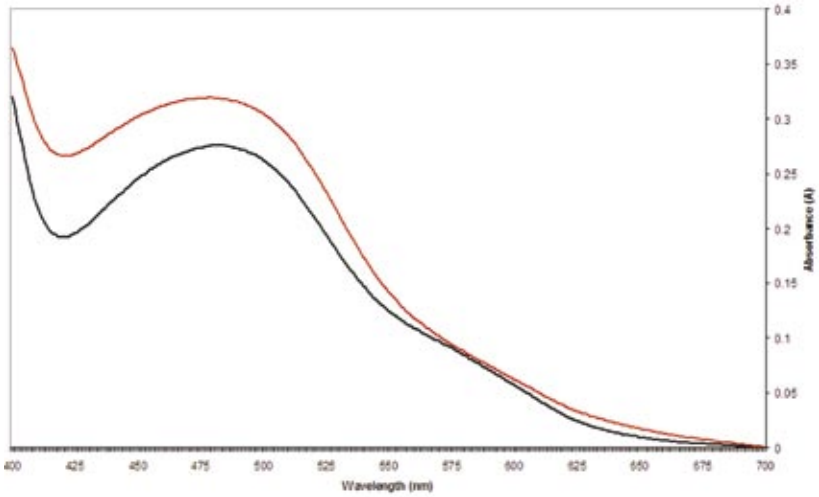

Figure 4: The UV-Vis spectra of a 15 µm thick membrane containing CR-546 in an aqueous environment (black line) and in a 20% ethanol environment (red line) are shown. Literature shows a much more defined peak for the unreacted dye compared to the small shoulder, which was observed experimentally.[10] These spectra were used to find the change in absorbance for use in modeling with the Kramers-Kronig equation, which gave a resulting Δn of 3×10^{-5}, which was too small to observe resonance effects.

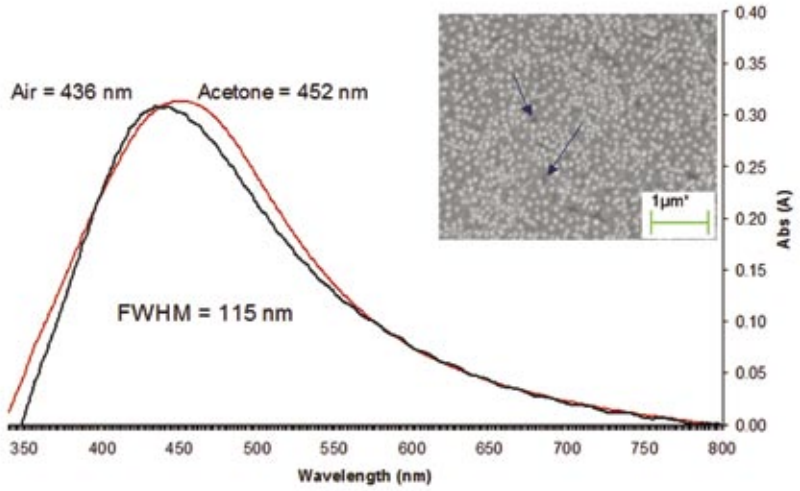

Figure 5: UV-Vis spectra show broad quadrupolar peaks from immobilized silver nanospheres in PDMS in the atmosphere (black line) and in acetone (red line). Both peaks were ~4 times broader than previously reported quadrupolar peaks because of lower surface density. The inserted SEM image shows this nonideal surface density emphasized by the arrows. These spectra were used in Kramers-Kronig modeling, resulting in a promising Δn of 0.02.

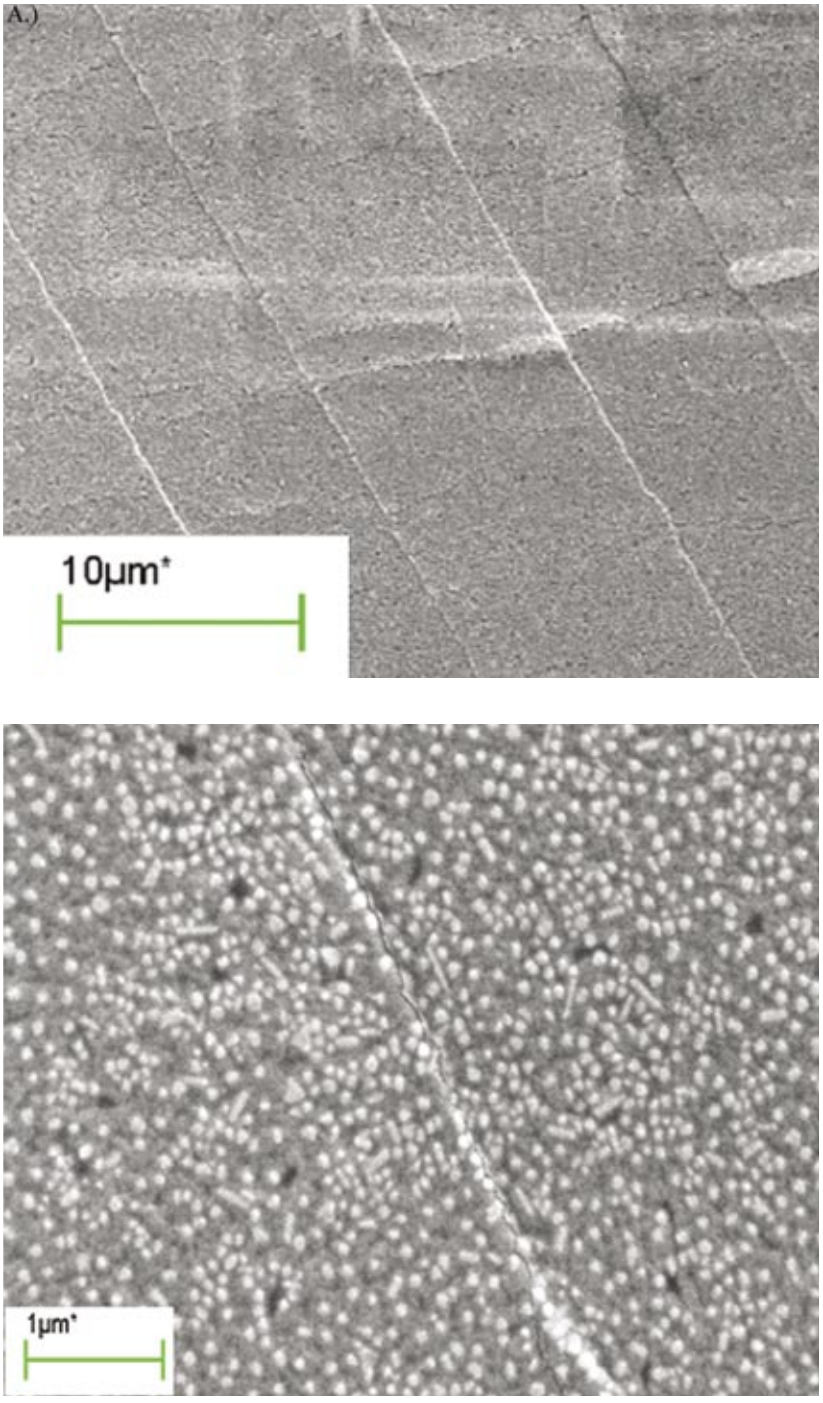

Figure 6: 6A shows an SEM image of a PDMS grating, patterned into channels with a height difference of ~60 nm. Magnification of this pattern (6B) shows that the spheres are present in and out of the channels. In order to obtain better refractive index contrast, the spheres would be present at only one height or formation of a grating based solely on the location of the unpatterned spheres.

The UV-Vis spectra of the immobilized spheres were taken, as shown in Figure 5. The full width half max values (FWHM) in these spectra were ~115 nm, which is ~4 times the FWHM shown in reference 12. Regardless, a 16 nm shift (λ_{max} 436 to 452 nm) in absorbance due to acetone exposure was observed, also shown in Figure 5. This shift was still great enough to yield a predicted Δn of 0.02, which should be large enough to produce resonance amplification.

Attempts to fabricate PDMS gratings with immobilized silver nanospheres were successful, as shown by the SEM images in Figure 6a and 6b, which also show that surface density could be increased. The depth of the grating is not known; however, it can be assumed to be approximately equal to the depth of the silicon master, which was 63 nm. Time restrictions did not allow the fabrication of a better diffraction grating, in which the spheres would be within quadrupolar coupling distances in channels separated from other sphere channels.

Conclusions

Two attempts at signal enhancement based on optical resonance in diffraction-based sensing were made. The first approach, incorporating the chromoreatand dye CR-546 into the grating, was abandoned due to modeling-predicted small amplification effects. The second approach, immobilizing silver nanospheres in PDMS, gave promising results based on shifts in the quadrupolar extinction peak. Future work includes increasing the surface coverage to obtain a narrower quadrupolar peak and fabricating a grating consisting of channels patterned from the silver nanospheres.

References

(1) Bailey, R. C.; Parpia, M. O.; Hupp, J. T. *Materials Today* **2005,** *8(4)*, 46–52.

(2) St. John, P. M.; Davis, R.; Cady, N.; Czajka, J.; Batt, C. A.; Craighead, H. G. *Anal. Chem.* **1998,** *70*, 1108–1111.

(3) Morhard, F.; Pipper, J.; Dahint, R.; Grunze, M. *Sensors and Actuators B* **2000,** *70*, 232–242.

(4) Goh, J. B.; Tam, P. L.; Loo, R. W.; Goh, M. *Anal. Biochem.* **2003,** *313*(2), 262–266.

(5) Nakajima, F.; Hirakawa, Y.; Kaneta, T.; Imasaka, T. *Anal. Chem.* **1999,** *71*, 2262–2265.

(6) Bailey, R. C.; Hupp, J. T. *Anal. Chem*. **2003,** *75*, 2392–2398.

(7) Bailey, R. C.; Hupp, J. T. J. *Am. Chem. Soc*. **2002,** *124*, 6767–6774.

(8) Schanze, K. S.; BergStedt, T. S.; Hauser, B. T.; Cavalaheiro, C. S. P. *Langmuir* **2000,** *16*, 795–810.

(9) Mohr, G. J.; Citterio, D.; Spichiger-Keller, U. E. *Sensors and Actuators B* **1998,** *49*, 226–234.

(10) Mohr, G. J. *Anal. Chim. Acta* **2003,** *508*, 233–237.

(11) Chumanov, G.; Sokolov, K.; Cotton, T. M. J. *Phys. Chem.* **1996,** *100*, 5166–5168.

(12) Chumanov, G.; Malynych, S. J. *Am. Chem. Soc.* **2003,** *125*, 2896–2898.

(13) Lee, P. C.; Meisel, D. J. *Phys. Chem.* **1982,** *88*, 3391–3395.

(14) Evanoff, D. D.; Chumanov, G. J. *Phys. Chem. B* **2004,** *108*, 13948–13956.

(15) Dang, X.; Stevenson, K. J.; Hupp, J. T. *Langmuir* **2001,** *17*, 3109–3112.